Proc. Natl. Acad. Sci. USA
Vol. 91, pp. 12847–12851, December 1994
Biochemistry

Construction of a bisaquo heme enzyme and binding by exogenous ligands

D. E. McRee, G. M. Jensen, M. M. Fitzgerald, H. A. Siegel, and D. B. Goodin*

Department of Molecular Biology, MB8, The Scripps Research Institute, 10666 North Torrey Pines Road, La Jolla, CA 92037

Communicated by Jane S. Richardson, September 22, 1994 (received for review June 23, 1994)

ABSTRACT **The crystal structure of the His-175 → Gly (H175G) mutant of cytochrome-*c* peroxidase (EC 1.11.1.5), missing its only heme ligand, reveals that the histidine is replaced by solvent to give a bisaquo heme protein. This protein retains some residual activity, which can be stimulated or inhibited by addition of exogenous ligands. Structural analysis confirms the binding of imidazole to the heme at the position of the wild-type histidine ligand. This imidazole complex reacts readily with hydrogen peroxide to produce a radical species with novel properties. However, reactivation in this complex is incomplete (≈5%), which, in view of the very similar structures of the wild-type and the H175G/imidazole forms, implies a critical role for tethering of the axial ligand in catalysis. This study demonstrates the feasibility of constructing heme enzymes with no covalent link to the protein and with unnatural ligand replacements. Such enzymes may prove useful in studies of electron transfer mechanisms and in the engineering of novel heme-based catalysts.**

The parameters required of the axial ligands for defining the diverse chemistry of heme enzymes are elusive. Peroxidases often contain a histidine ligand to the iron, whereas cysteine is found in monooxygenases and tyrosine in catalases (1, 2). Cytochrome-*c* peroxidase (CCP; EC 1.11.1.5) catalyzes the oxidation of cytochrome *c* (cyt *c*) by H_2O_2 through an intermediate state (ES) that consists of a ferryl (Fe^{4+}=O) heme and a free radical localized on Trp-191 (3). The buried carboxylate of Asp-235 stabilizes this free radical and also accepts a hydrogen bond from the histidine heme ligand, His-175. The resulting Asp/His/metal triad is a common motif in metalloproteins and is reminiscent of the Asp/His/Ser triad of serine proteases (4, 5). In this study, we report the deletion of the histidine iron ligand of CCP to produce a heme enzyme which contains no covalent link to the protein. The facile occupation of this cavity by exogenous small molecules demonstrates the potential for producing heme catalysts containing a wide range of unnatural ligands.

MATERIALS AND METHODS

Protein Expression and Purification. Wild-type and mutant CCP proteins were overexpressed in *Escherichia coli* BL21(DE3) using the plasmid pT7CCP (6). Wild-type CCP in our laboratory is that with Met-Lys-Thr at the N terminus and containing Ile-53 and Gly-152 (7). The His-175 → Gly (H175G) mutant was created by site-directed mutagenesis, expressed, purified to homogeneity, and reconstituted with heme as described (6). This purified reconstituted protein was crystallized twice against distilled water and stored as a crystal suspension at 77 K. Protein concentrations were determined from the extinction coefficients determined by pyridine hemochromogens (8, 9). In the case of H175G the extinction coefficient was determined for the 280-nm band because of the variability (with pH and temperature) in the intensity and energy of the Soret band (see below).

X-Ray Crystallography.† Attempts to obtain crystals of H175G by vapor diffusion against 30% 2-methyl-2,4-pentanediol were unsuccessful. However, successive rounds of crystallization against distilled water yielded single crystals of sufficient quality for structure determination. The space group ($P2_12_12_1$, a = 105.2 Å, b = 74.3 Å, and c = 45.4 Å) was identical to a form of CCP grown from 30% 2-methyl-2,4-pentanediol (9). For H175G/imidazole (Im), the mother liquor was replaced with 5 mM imidazole (pH 7.0) for 20 min before mounting. Each data set was collected from a single crystal on a Mar Research (Hamburg, Germany) image plate (d = 100 mm) with an oscillation angle of 1° for 120 images, utilizing a GX21 rotating anode operating at 40 kV and 70 mA with a 0.3-mm focus and Franks focusing mirrors. Data for H175G and H175G/imidazole were integrated with the program XDS (10) and merged and scaled with data for wild-type CCP (9), and $(|F_{mutant}| - |F_{native}|)\alpha_{native}$ difference Fourier maps made with the program system XTALVIEW (11). As the H175G/imidazole map gave the smallest difference density, this structure was refined first, followed by solution of the H175G structure, using the refined structure of H175G/imidazole as the initial model. The most significant features in the H175G/imidazole map included a strong negative peak corresponding to the loss of the histidyl C^β atom and features indicating a shift of main-chain atoms of residues 175 and 176. Other small differences on the surface of the protein could be interpreted as changes in the water structure and surface side-chain orientations, possibly as a result of the different crystallization conditions. An imidazole ring was placed into the density and refined by using XPLOR (Axel Brünger, Yale University) with least-squares conjugate gradient and B-value refinement. Several rounds of refinement were alternated with manual adjustment of the model. The final H175G/imidazole model, with the imidazole removed, was used as the starting model for the H175G structure without added ligand. After the first round of refinement, three water molecules were added to the proximal cavity at the observed peak positions before further refinement.

Spectroscopy and Kinetics. UV/visible absorption spectra were obtained on a Hewlett–Packard model 8452A diode-array spectrophotometer. EPR spectra were obtained on a Bruker (Billerica, CA) model ESP300 spectrometer equipped with an Air Products and Chemicals (Allentown, PA) model LTR3 liquid helium cryostat. Steady-state kinetics for the CCP-catalyzed oxidation of yeast cyt *c* by H_2O_2 at 23°C were determined in 200 mM potassium phosphate buffer (pH 7.0) as described (7, 12). Values of k_{obs} are expressed in terms of enzyme turnover/sec at a single cyt *c* concentration, 25 μM,

The publication costs of this article were defrayed in part by page charge payment. This article must therefore be hereby marked "*advertisement*" in accordance with 18 U.S.C. §1734 solely to indicate this fact.

Abbreviations: CCP, cytochrome-*c* peroxidase; cyt *c*, cytochrome *c*; Im, imidazole; *N*-MeIm, *N*-methylimidazole; $[Fe(TPP)(OH_2)_2]^+$ diaquo[*meso*-tetraphenylporphinato]iron(III).

*To whom reprint requests should be addressed.

†Atomic coordinates of H175G CCP and H175G/imidazole CCP have been deposited in the Brookhaven Protein Data Bank (file nos. ICCE and ICCG, respectively).

Table 1. Diffraction data collection and refinement statistics

	H175G	H175G/Im
Total reflections	86,869	86,150
Unique reflections	17,907	18,373
Reflections used for refinement	12,701	15,000
Resolution range, Å	7.0–2.3	5.0–2.1
Completeness of data	91%	94%
R_{sym}	0.105	0.051
R_{cryst}	0.191	0.193
rms_{bond}, Å	0.015	0.016
rms_{angle}	3.1°	3.1°

Only reflections between the stated resolution with $I/\sigma_I > 2.0$ were used for refinement. $R_{cryst} = \Sigma(F_o - F_c)/\Sigma(F_o)$; $R_{sym} = \Sigma(I_h - \bar{I}_h)/\Sigma I_h$; rms_{bond} and rms_{angle} give the root-mean-squared deviation between the observed and ideal values.

and H_2O_2 concentration, 100 μM, which are near saturating conditions for wild-type CCP. Im and *N*-methylimidazole (*N*-MeIm) were added to 10 mM where indicated. Enzyme concentrations were varied to maintain a roughly constant rate of change in absorbance. Uncertainty in measurements of k_{obs} are estimated at ±3%. Im binding at 24°C and pH 7.0 was measured by optical titration. Values of K_d were determined from the heme Soret absorbance change at 412 nm (Im), or 414 nm (*N*-MeIm) by assuming one binding site per molecule. Weaker binding by *N*-MeIm prevented the precise determination of its K_d value. Spin integrations of the free-radical signal were determined from EPR at 7 K after mixing 1.5 molar equivalents of H_2O_2 with 105 μM CCP in 100 mM potassium phosphate (pH 7) in the absence or presence of 50 mM Im. The [free radical]/[protein] values for the H175G species are underestimated, because the sample was frozen ≈20 sec after oxidation, but the signals were observed to completely decay within several minutes. Instrument conditions were 2-mM microwave power at 9.51 GHz, with 100-kHz field modulation at 5-G amplitude.

RESULTS AND DISCUSSION

The crystal structure of H175G CCP at 2.3-Å resolution (Table 1; Fig. 1 *Upper Left*) shows that the heme is coordinated by two water molecules. The electron density for these solvent peaks (Fig. 1 *Upper Left*) contains two symmetric lobes on either side of the heme. One peak is observed at the

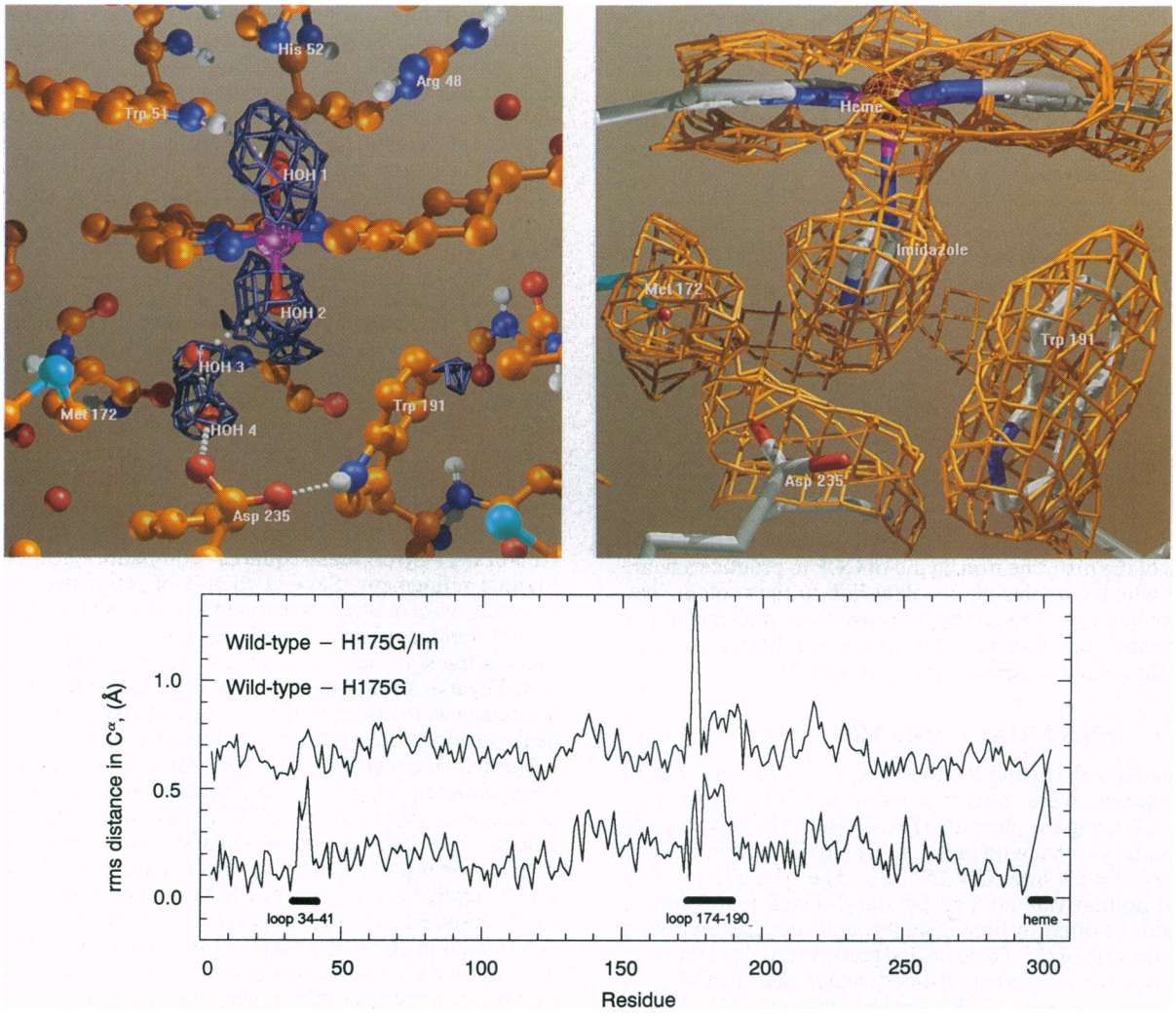

FIG. 1. X-ray crystal structures of H175G and its Im complex. (*Upper Left*) $|F_o| - |F_c|$ omit map of the 2.3-Å structure of H175G superimposed on the refined model. The coordinating waters, HOH1 and HOH2, as well as two additional water molecules, HOH3 and HOH4, were omitted from the model before calculation of the omit electron density, shown contoured at 3σ. (*Upper Right*) $2|F_o| - |F_c|$ electron density map, contoured at 1σ, is superimposed upon the refined model of an H175G crystal after soaking in 5 mM Im. (*Bottom*) Plots of the rms difference in C^α positions between wild-type CCP (9) and the H175G structure (lower plot) and the difference between the wild-type and H175G/Im structures (upper plot, offset for clarity). For each plot, the last four points represent carbon atoms in the heme macrocycle. The coordinated movement of the heme and the surface loops from Ala-174 to Pro-190 and from Asp-34 to Gly-41 (marked by heavy lines) are observed only in the bisaquo state.

position of the His-175 N^{ϵ} atom of the wild-type enzyme, while the peak on the distal heme face is near the same position as the "weakly" coordinated water of the wild-type structure (13). Refinement of the H175G structure results in the placement of the iron atom in the plane of the heme, with the two Fe—O bonds at equal distances of 2.0 Å. Both of these observations are consistent with the structure of the bisaquo heme model complex diaquo[*meso*-tetraphenylporphinato]iron(III) perchlorate, $[Fe(TPP)(OH_2)_2]^+$ (14, 15). Two smaller peaks in the proximal cavity are modeled as water molecules with higher *B* factors. These waters form a network of hydrogen bonds that connect the heme, the carboxyl group of Asp-235, and the main-chain carbonyl of Met-172. The heme of H175G shifts slightly (≈0.5 Å) in its binding pocket in the direction of its propionate groups. In addition, the loops extending from Ala-174 to Pro-190 and from Asp-34 to Gly-41, which wrap around the heme propionates, shift with the heme (see Fig. 1 *Bottom*).

Soaking crystals of H175G in 5 mM Im results in a change in color from brown-green to red, consistent with its optical properties in solution (see below). The structure of the H175G/Im complex at 2.1-Å resolution (Table 1; Fig. 1 *Upper Right*) reveals that Im binds to the proximal cavity formerly occupied by the histidine. The coordinating nitrogen of the H175G/Im complex is in a position equivalent to the wild-type histidine N^{ϵ}, but the plane of the Im refines to a position which is tilted slightly (≈20°) relative to the wild-type histidyl ring. Im binding restores the heme and the loops contacting the heme propionate region to the positions observed for the wild-type enzyme (Fig. 1 *Bottom*). A difference remains at the site of the mutation, where the Gly-175 C^{α} has shifted by 0.7 Å toward the heme. Smaller changes are evident in the main-chain atoms of residues Ala-174 to Leu-177, but unlike the bisaquo protein, the main-chain atoms of the wild-type and H175G/Im structures reconverge after Gly-178. A small change in the position of Trp-191 is also observed, in which the C_{β} shifts by 0.4 Å. The structures of the H175G/Im complex and the wild-type enzyme are otherwise very similar.

Spectroscopic properties of the H175G mutant are consistent with bisaquo coordination and the return to a native-like state in the presence of imidazole. In the optical spectra of Fig. 2, the bisaquo H175G exhibits a broad Soret band with a maximum at 395 nm, similar to the $[Fe(TPP)(OH_2)_2]^+$ model complex (14, 15) and to the low-pH forms of myoglobin (16, 17) and cyt *c* (18), wherein loss of the protein ligands has been

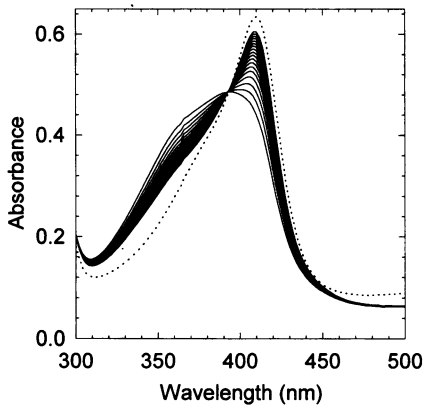

FIG. 2. Optical spectra of bisaquo H175G and its titration with Im. Absorbance spectra of 8 μM H175G in 100 mM potassium phosphate (pH 7.0) were collected at 24°C. The peak of the Soret band shifts from 390 nm for H175G in buffer alone to 408 nm with successive 1-μl additions of 1 M Im (pH 7) to 2900-μl samples. Isosbestic points occur at 382 nm and 302 nm. For comparison, the spectrum of wild-type CCP is also shown (dotted line).

proposed. Titration of the bisaquo H175G protein with Im at pH 7 results in a two-state conversion to a form with an optical spectrum that is essentially that of the high-spin ferric wild-type enzyme, with a Soret maximum at 408 nm (Fig. 2). The absence of αβ bands in the 530- to 570-nm range of these spectra indicates that both forms are in a high-spin ferric state (data not shown). The equilibrium dissociation constant (K_d) for Im as measured by the spectral change is 2.7 mM (Table 2). Electron paramagnetic resonance (EPR) spectra of H175G and wild-type CCP are compared in Fig. 3*a*. As isolated, the wild-type enzyme exhibits a high-spin ferric EPR signal with a small rhombic distortion (g_x = 6.56, g_y = 5.20) that is critically dependent on the geometry of axial ligand coordination (9, 20). The EPR spectrum of bisaquo H175G also reflects a high-spin ferric state but indicates that the protein is a mixture of axial ($g_{\perp}$ = 5.99) and rhombic (g_x = 6.59, g_y = 5.37) components (Fig. 3*a*). Axial high-spin ferric EPR was also observed in the bisaquo $[Fe(TPP)(OH_2)_2]^+$ complex (15). Upon addition of Im, H175G reverts to a single species which is similar to wild-type enzyme, albeit with a slightly smaller rhombic distortion (g_x = 6.55, g_y = 5.41).

The resting ferric state of H175G and its imidazole complex react with H_2O_2 to give an oxidized heme, and in the case of the Im complex, an unusual free-radical center is observed. The ferric EPR signals of wild-type CCP, H175G, and H175G/Im are lost upon oxidation by H_2O_2 and each of these oxidized proteins exhibit optical spectra consistent with a ferryl center (Fe^{4+}=O) (data not shown). However, the Trp-191 free-radical signal of wild-type CCP, with its characteristic anisotropy (21), was not observed for H175G (Fig. 3*b*). Instead, only a narrow, isotropic signal integrating to ≈0.1 spin per enzyme was observed. At present we are unable to assign this radical, but similar signals, unassociated with Trp-191, are often seen in inactive mutants of CCP (12, 19, 22). In contrast, reaction of the H175G/Im complex with H_2O_2 gives rise to a broad EPR signal with apparent axial symmetry which integrates to ≈0.3 spin per enzyme. The line-shape of this signal is distinctly dissimilar to the Trp-191 free radical of wild-type CCP in that the broad shoulder appears to higher field of the main signal (see Fig. 3*b*). Houseman *et al.* (21) have shown that the lineshape of the Trp-191 free radical may result from a very weak exchange coupling between the radical and ferryl heme, so that small deviations in conformation result in averaging over ferromagnetic and antiferromagnetic couplings of the centers. As observed with another proximal mutant, D235E, small changes in conformation can significantly alter the free-radical lineshape (9). The small change in the position of Trp-191 observed for the H175G/Im complex is consistent with these interpretations.

H175G retains residual activity in the oxidation of cyt *c*, and this activity can be stimulated or inhibited depending upon the nature of the added exogenous ligand. In the bisaquo state, H175G is 1.6% as active as the wild-type enzyme (Table 2), indicating that the network of solvent in the proximal cavity is able partially to serve the function of the axial ligand. In the

Table 2. Activity, Im binding, and free-radical quantitation of H175G

CCP	k_{obs}, sec^{-1}	Activity, %	K_d, mM	[Free radical]/[protein]
WT	570	100	—	1.0
H175G	9	1.6	—	0.1
WT + Im	823	100	—	—
H175G + Im	37	4.5	2.7	0.3
WT + *N*-MeIm	634	100	—	—
H175G + *N*-MeIm	3	0.5	>20	—

WT, wild type.

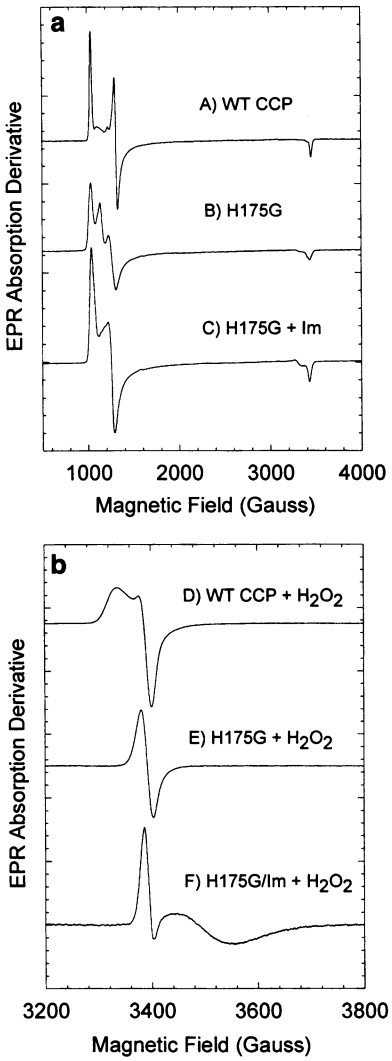

FIG. 3. EPR spectra at 7 K for resting (*a*) and H_2O_2-oxidized (*b*) H175G. Trace A: high-spin ferric iron signals for wild-type (WT) CCP showing the small rhombic distortion with $g_x = 6.56$, $g_y = 5.20$. Trace B: bisaquo H175G in the high-spin ferric resting state is a mixture of a rhombic species with $g_x = 6.59$, $g_y = 5.37$ and an axial species with $g_\perp = 5.99$. Trace C: In the presence of Im, H175G reverts to a single species with a slightly smaller rhombic distortion ($g_x = 6.55$, $g_y = 5.41$) than observed for wild-type enzyme. Trace D: the Trp-191 free-radical signal of wild-type CCP with $g_{\perp(\text{apparent})} = 2.01$ and $g_{\|(\text{apparent})} = 2.03$. Trace E: the isotropic signal arising from the oxidation of bisaquo H175G with 1.5 equivalents of H_2O_2; the signal might not arise from Trp-191, because it is similar to that observed for a number of mutants lacking this residue (12, 19). Trace F: the broad free-radical signal observed for the H175G/Im complex after oxidation with 1.5 equivalents of H_2O_2 exhibits an apparent axial lineshape with $g_{\perp(\text{apparent})} = 2.00$ and $g_{\|(\text{apparent})} = 1.92$. The unusual lineshape may be due to a subtle change in the distribution of exchange couplings between the free radical and ferryl (Fe^{4+}=O) heme, due to small changes in the linkage of proximal groups. Protein concentrations were 150 μM CCP in 100 mM potassium phosphate (pH 7) in the absence or presence of 50 mM Im. Instrument conditions: 2-mW microwave power at 9.51 GHz, with 100-kHz field modulation at 5-G amplitude.

presence of 10 mM Im, the enzyme turnover is increased to 4.5% of the wild-type activity under the same conditions. While this stimulation is significant, it is remarkable that the activity is not higher, in view of the structural similarity of the H175G/Im complex to the native enzyme. It is possible that the small changes observed in the orientations of the imidazole, other proximal atoms, or changes not observable at 2.1-Å resolution are responsible for the lack of full activity. However, an intriguing possibility is that the reduced enzyme turnover is due to the loss of the ligand tether to the backbone at position 175. Although a report of the H175Q mutant of CCP, which retains full activity, has called into question the importance of the axial ligand to function (23, 24), it is possible that the activity of H175Q may owe significantly to its covalent tether to the protein. Such a tether could be important to enzyme function in several ways, including restriction of iron movement into the heme plane upon reaction with H_2O_2, allosteric communication through position 175, reducing the multiplicity of side-chain conformation, or in providing a covalent link in an important electron transfer pathway. The H175Q mutant also retains a hydrogen bond to Asp-235 (23, 24), an interaction that critically modulates the properties of the heme (9). Importantly, *N*-MeIm, which cannot simultaneously coordinate the heme and participate in a hydrogen-bond with Asp-235, further inhibits the basal activity of H175G to 0.5% of wild type (Table 2). This indicates that the H175G/Im complex, functionally compromised as it is, gains catalytic advantage from the hydrogen bond to Asp-235. Therefore, these studies together have shown that an Im ligand is neither necessary nor sufficient for efficient function of CCP. The critical features most likely reside with the nature of the Fe–ligand bond, geometrical constraints of the iron with respect to the heme plane, and/or in a covalent connection to the protein.

Some proteins appear to tolerate the deletion of buried residues to form cavities which can serve as small molecule binding sites (6, 25). While the removal of metalloprotein ligands can result in the deleterious loss of cofactor binding, the recruitment of nearby residues as surrogate ligands has also been observed (26). For several proteins, including azurin (27), cyt *c* (28), and myoglobin (29, 30), deletion of one of the metal ligands has resulted in the assembly of ligand-deficient metal cofactors which can coordinate exogenous small molecules. The bisaquo H175G mutant of CCP represents a case of a heme enzyme without any covalent linkage to the protein, a result which may have important implications for studies of the mechanism of electron transfer pathways in proteins (31). In addition, binding of exogenous ligands to the bisaquo heme opens many avenues for the study of a host of ligands unavailable by site-directed mutagenesis. By introducing substituted imidazoles, thiolates, carboxylates, amines, or alcohols into an untethered heme protein, a diverse set of heme enzymes may be created to mimic the monooxygenases, hydroxylases, or catalases. It is also likely that ligands such as NO, CO, CN, SCN, halides, or heterocyclic ligands without analogs to natural amino acids will offer routes for completely novel chemistry within an artificial heme enzyme.

We thank Professor S. Boxer for communicating results prior to publication and W. Chazin, R. Ghadiri, H. B. Gray, S. Redford, C. D. Stout, S. Wilcox, and P. Wright for helpful discussions. This research was supported by Grants GM41049 (to D.B.G.) and GM15733 (to M.M.F.) from the National Institutes of Health.

1. Dawson, J. H. (1988) *Science* **240**, 433–439.
2. Poulos, T. L. (1988) *Adv. Inorg. Biochem.* **7**, 1–33.
3. Sivaraja, M., Goodin, D. B., Smith, M. & Hoffman, B. M. (1989) *Science* **245**, 738–740.
4. Warshel, A., Naray-Szabo, G., Sussman, F. & Hwang, J.-K. (1989) *Biochemistry* **28**, 3629–3637.
5. Christianson, D. W. & Alexander, R. S. (1989) *J. Am. Chem. Soc.* **111**, 6412–6419.
6. Fitzgerald, M. M., Churchill, M. J., McRee, D. E. & Goodin, D. B. (1994) *Biochemistry* **33**, 3807–3818.
7. Goodin, D. B., Davidson, M. G., Roe, J. A., Mauk, A. G. & Smith, M. (1991) *Biochemistry* **30**, 4953–4962.

8. Nicola, N. A., Minasian, E., Appleby, C. A. & Leach, S. J. (1975) *Biochemistry* **14,** 5141–5149.
9. Goodin, D. B. & McRee, D. E. (1993) *Biochemistry* **32,** 3313–3324.
10. Kabsch, W. (1988) *J. Appl. Crystallogr.* **21,** 916–924.
11. McRee, D. E. (1992) *J. Mol. Graphics* **10,** 44–46.
12. Goodin, D. B., Mauk, A. G. & Smith, M. (1987) *J. Biol. Chem.* **262,** 7719–7724.
13. Finzel, B. C., Poulos, T. L. & Kraut, J. (1984) *J. Biol. Chem.* **259,** 13027–13036.
14. Kastner, M. E., Scheidt, W. R., Mashiko, T. & Reed, C. A. (1978) *J. Am. Chem. Soc.* **100,** 666–667.
15. Scheidt, W. R., Cohen, I. A. & Kastner, M. E. (1979) *Biochemistry* **18,** 3546–3552.
16. Sage, J. T., Morikis, D. & Champion, P. M. (1991) *Biochemistry* **30,** 1227–1237.
17. Traylor, T. G., Deardruff, L. A., Coletta, M., Ascenzi, P., Antonini, E. & Brunori, M. (1983) *J. Biol. Chem.* **258,** 12147–12148.
18. Lanir, A. & Avirim, I. (1975) *Arch. Biochem. Biophys.* **166,** 439–445.
19. Fishel, L. A., Farnum, M. F., Mauro, J. M., Miller, M. A., Kraut, J., Liu, Y. J., Tan, X. L. & Scholes, C. P. (1991) *Biochemistry* **30,** 1986–1996.
20. Smith, T. D. & Pilbrow, J. R. (1980) in *Biological Magnetic Resonance*, eds. Berliner, L. J. & Jacques, R. (Plenum, New York), pp. 85–168.
21. Houseman, A. L. P., Doan, P. E., Goodin, D. B. & Hoffman, B. M. (1993) *Biochemistry* **32,** 4430–4443.
22. Hori, H. & Yonetani, T. (1985) *J. Biol. Chem.* **260,** 349–355.
23. Sundaramoorthy, M., Choudhury, K., Edwards, S. L. & Poulos, T. L. (1991) *J. Am. Chem. Soc.* **113,** 7755–7757.
24. Choudhury, K., Sundaramoorthy, M., Mauro, J. M. & Poulos, T. L. (1992) *J. Biol. Chem.* **267,** 25656–25659.
25. Eriksson, A. E., Baase, W. A., Wozniak, J. A. & Matthews, B. W. (1992) *Nature (London)* **355,** 371–373.
26. Martin, A. E., Burgess, B. K., Stout, C. D., Cash, V. L., Dean, D. R., Jensen, G. M. & Stephens, P. J. (1990) *Proc. Natl. Acad. Sci. USA* **87,** 598–602.
27. Denblauwen, T. & Canters, G. W. (1993) *J. Am. Chem. Soc.* **115,** 1121–1129.
28. Lu, Y., Casimiro, D. R., Bren, K. L., Richards, J. H. & Gray, H. B. (1993) *Proc. Natl. Acad. Sci. USA* **90,** 11456–11459.
29. Barrick, D. (1994) *Biochemistry* **33,** 6546–6554.
30. DePillis, G. D., Decatur, S. M., Barrick, D. & Boxer, S. G. (1994) *Biophys. J.* **66,** A400 (abstr.).
31. Beratan, D. N., Onuchic, J. N., Winkler, J. R. & Gray, H. B. (1992) *Science* **258,** 1740–1741.